

Phase Diagram of Na_xCoO_2 Studied by Gutzwiller Density Functional Theory

Guang-Tao Wang¹, Xi Dai¹, Zhong Fang¹

¹*Beijing National Laboratory for Condensed Matter Physics,
and Institute of Physics, Chinese Academy of Sciences, Beijing 100080, China*

(Dated: November 3, 2018)

The ground states of Na_xCoO_2 ($0.0 < x < 1.0$) is studied by the LDA+Gutzwiller approach, where charge transfer and orbital fluctuations are all self-consistently treated *ab-initio*. In contrast to previous studies, which are parameter-dependent, we characterized the phase diagram as: (1) Stoner magnetic metal for $x > 0.6$ due to a_{1g} van-Hove singularity near band top; (2) correlated non-magnetic metal without e'_g pockets for $0.3 < x < 0.6$; (3) e'_g pockets appear for $x < 0.3$, and additional magnetic instability involves. Experimental quasi-particle properties is well explained, and the a_{1g} - e'_g anti-crossing is attributed to spin-orbital coupling.

PACS numbers: 71.20.-b, 71.27.+a

Transition-metal oxides have complex phase diagrams due to the interplay between the charge, spin and orbital degrees of freedom. Among them Na_xCoO_2 is a typical system showing doping-dependent phase control [1]. It has been found experimentally as non-magnetic (NM) metal for Na poor side, while Curie-Weiss metal for Na rich side [1, 2], and A-type (layered) anti-ferromagnetic (AF) state for $x \sim 0.75$ [3]. In addition, superconductivity is discovered for hydrated $\text{Na}_x\text{CoO}_2 \cdot y\text{H}_2\text{O}$ ($x \sim 0.35$) [4], and charge-spin-orbital ordered states are suggested for $x = 0.5$ due to Na ordering [5]. The rich properties of Na_xCoO_2 attract much of the research interests due to not only its potential applications, but also the challenging theoretical issues in this system generated by both the *multi-orbital* nature and strong e-e correlation.

Na_xCoO_2 is crystallized in planar triangle lattice, with each Co site being coordinated by edge-shared oxygen-octahedron. The e_g states are about 2eV higher than t_{2g} , and the Fermi level is located within the Co- t_{2g} multiplet, which splits again into one a_{1g} and two e'_g orbitals under trigonal crystal field. For Na concentration x , the effective number of t_{2g} electrons per Co is given as $5+x$, and thus the low energy physics here is dominated by the multiple orbits ($a_{1g}+e'_g$), where charge, spin and orbital degrees of freedom are all active. The rigorous computational tools for such systems are still lacking, and the observed rich phenomena remains far from even qualitative being understood. The main controversial issues are: (1) for $x = 0.3$, are there any Fermi surface pockets for the e'_g band? These pockets are predicted by LDA (local density approximation) calculations [6] but not observed by ARPES [7]. (2) Is the $x > 0.5$ side more “correlated” than $x < 0.5$ side, as suggested by the Curie-Weiss behavior for the Na rich side? It is expected from simple band picture that $x = 1.0$ end compound is a band insulator rather than Mott insulator.

Both LDA and LDA+ U methods fail for such system due to the insufficient treatment of electron correlation. This is why many issues look controversial following the LDA pictures. For instances, LDA predicts ferromag-

netic metal as the ground state for the whole doping region, and LDA+ U even enhances the tendency to be ferromagnetic [8]; the band width obtained by LDA or LDA+ U is about two times larger than what observed by ARPES [9]; the e'_g pockets problem as mentioned above; and etc. To treat the electron correlation more precisely, the Gutzwiller [10] and DMFT (dynamic mean field theory) [11] approaches has been adopted, where fluctuation effects are included. However, those studies are only focused on the $x = 0.3$ compound using tight-binding Hamiltonian extracted from LDA, and conflicting results are drawn due to different parameters [12].

In this paper, we show that the above mentioned theoretical challenging issues of this multi-orbital correlated electron systems can be well studied by using the recently developed LDA+Gutzwiller method [13], which keeps the parameter-free character of density functional theory (DFT) and includes all possible charge transfer and orbital fluctuation effects self-consistently. As the results, a phase diagram for the whole doping region is constructed, which removes away most of the above mentioned controversial issues, and suggests that physics here dominates by the doping-dependent orbital, charge and spin fluctuations.

To overcome the problem of LDA, the common procedure of LDA+ U and DMFT schemes [15] are to draw out from the LDA Hamiltonian the interaction terms for the localized orbitals, such as the $3d$ or $4f$ states, and then treat the interaction Hamiltonian explicitly in a proper way (beyond LDA). The total Hamiltonian reads:

$$\begin{aligned} H^{LDA+G} &= H^{LDA} + H_{int} - H_{dc} \\ H_{int} &= U \sum_{i\alpha} n_{i\alpha}^\uparrow n_{i\alpha}^\downarrow + \frac{U'}{2} \sum_{\substack{\alpha \neq \beta \\ i, \sigma, \sigma'}} n_{i\alpha}^\sigma n_{i\beta}^{\sigma'} - \frac{J}{2} \sum_{i\sigma, \alpha \neq \beta} n_{i\alpha}^\sigma n_{i\beta}^\sigma \\ < H_{dc} >^{LDA} &= \bar{U} N(N-1) - \frac{\bar{J}}{2} \sum_{\sigma} [N^\sigma(N^\sigma - 1)] \end{aligned} \quad (1)$$

where $|i\alpha\rangle^\sigma$ are a set of local orbitals with spin index σ

and occupation number $n_{i\alpha}$ for lattice site i ; the U, U' and J gives the intra-, inter-orbital repulsive interaction and Hund's exchange coupling, respectively. The H_{dc} is the double counting term from LDA, where interaction strength \bar{U} and \bar{J} are averaged over orbitals.

If the interaction term is treated by the Hartree-like scheme (LDA+ U), the correction over LDA is a set of energy shift of the local orbitals, leaving the kinetic part unchanged. This is fine if the fluctuation effect is not strong, but will fail in opposite case, such as the Na_xCoO_2 system studied here. In this sense, the DMFT method, in which frequency-dependent self-energy is properly computed, is much better than LDA+ U . However, due to the heavy computational cost for multi-orbital systems, the current DMFT studies [11, 12] are all applied to tight-binding Hamiltonians extracted from LDA without full charge density self-consistency. This is insufficient if the charge, spin and orbital degrees of freedom are all active as discussed above for Na_xCoO_2 .

In the LDA+Gutzwiller approach [13], the Gutzwiller wave function $|\Psi_G\rangle = \hat{P}|\Psi_0\rangle$ (\hat{P} is a projection to many-body configuration) is used instead of single Slater determinant wave function $|\Psi_0\rangle$. The orbital, charge and spin fluctuations can be included by the multi-configuration nature of the Gutzwiller wave function. As the results, a set of orbital-dependent kinetic energy renormalization factor Z_α are obtained for the correlated states in addition to the on-site energy shift. Unlike the previous Gutzwiller or DMFT studies [10, 11, 12], here all charge transfer processes, crystal field and orbital fluctuations are self-consistently treated within the framework of DFT, which allows for the accurate computation of ground state total energy.

We use the plane-wave pseudo-potential method, and choose the Co-3d Wannier functions as the correlated local orbitals. The atomic-limit convention $U = U' + 2J$ is followed. How to determine the value of U and J is a common problem for LDA+ U , DMFT and present methods, and no unified way is established yet. Nevertheless, reasonable estimations have been done for $U = 3.0 \sim 5.0\text{eV}$ and $J \sim 1.0\text{eV}$ for Na_xCoO_2 system following the literatures [10, 11]. Instead of using single fixed U , various values have been studied, and our qualitative results are not changed, as shown below. In addition, since our main purpose is to establish a general picture for the physics of Na_xCoO_2 , the structure differences among different doping x are neglected, and the Na doping is treated by virtual crystal approximation (therefore the charge-ordered states with Na ordering at particular doping, which is interesting but not our purpose here, is out of the phase diagram).

Fig.1 shows the phase diagram computed for the whole doping range $0.0 < x < 1.0$. The solid lines and the dashed lines represent the stabilization energies of FM state and layer-type AF state relative to NM solution, respectively. The intra-plane AF state is hard to be stabilized due

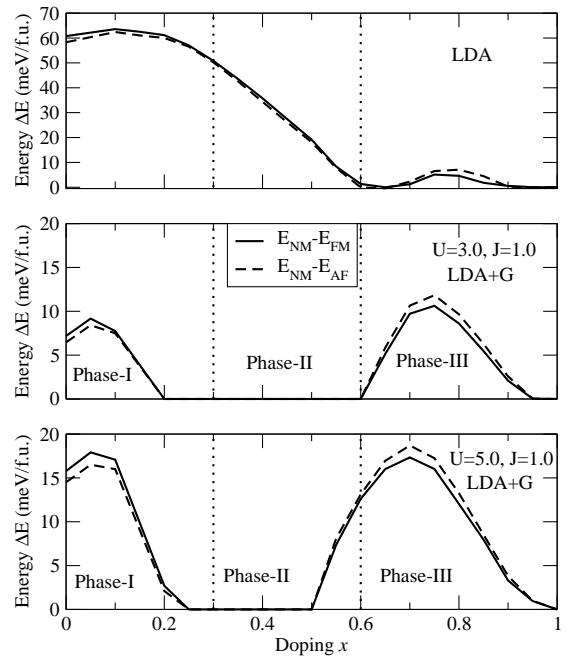


FIG. 1: The calculated stabilization energies of FM (solid lines) and layer-type AF (dashed lines) states with respect to NM state for Na_xCoO_2 over the whole doping range $0.0 < x < 1.0$. (a) Results obtained by LDA; (b) LDA+Gutzwiller results obtained using $U = 3.0$ eV and $J = 1.0$ eV; (c) LDA+Gutzwiller results obtained using $U = 5.0$ eV and $J = 1.0$ eV.

to geometrical fluctuation of triangle lattice. The LDA (shown in Fig.1(a)) gives magnetic ground states for all doping x , which are inconsistent with experiments. In contrast, the phase diagram by LDA+Gutzwiller has three distinct regions, which can be understood as the consequence of competition among crystal field splitting, inter-orbital charge and spin fluctuation, as discussed in the following parts. As shown in Fig.1(b) and (c), the features of phase diagram are qualitatively the same using $U = 3.0$ eV or $U = 5.0$ eV.

Phase II: correlated non-magnetic metal ($0.3 < x < 0.6$).

First of all, the NM state is now correctly predicted for this region. It is known that LDA overestimates the tendency to be FM for several systems, such as ruthenates [16], and this artifact is even enhanced by LDA+ U . The physical reason is that correlation effect is not properly treated in LDA and LDA+ U , but it is well included in the present formalism. In Fig.2 we summarize the properties of the NM solutions for the whole doping range. For x larger than 0.3, as shown in Fig.2 (a), the e'_g bands are fully occupied and the inter-orbital fluctuation (defined as F and S, see caption of Fig.2) is weak, indicating an effective single band system. However with x approaching the phase boundary around $x_c = 0.3$, a crossover to multi-band behavior has been detected from the strong inter-orbital spin and charge fluctuation as

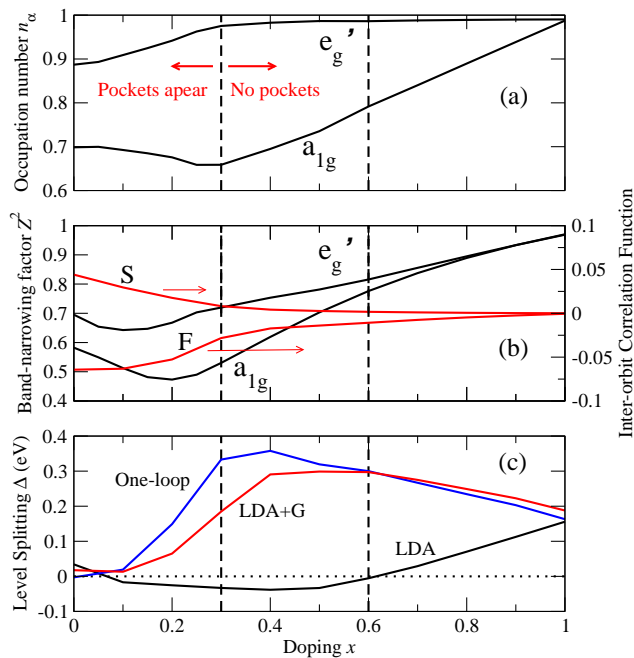


FIG. 2: Results for NM state as the functions of doping x with $U=5.0\text{eV}$ and $J=1.0\text{eV}$. (a) Occupation numbers; (b) Band renormalization Z_α^2 -factors, inter-orbit charge fluctuation $F=\langle \hat{n}_{a_{1g}} \hat{n}_{e'_g} \rangle - \langle \hat{n}_{a_{1g}} \rangle \langle \hat{n}_{e'_g} \rangle$, inter-orbit spin fluctuation $S=\langle \hat{S}_{a_{1g}}^z \hat{S}_{e'_g}^z \rangle - \langle \hat{S}_{a_{1g}}^z \rangle \langle \hat{S}_{e'_g}^z \rangle$; and (c) Level splitting $\Delta = \varepsilon_{a_{1g}} - \varepsilon_{e'_g}$.

shown in Fig.2(b). Such fluctuations in low doping area is induced by the Hund's rule coupling, which favors even distribution of electrons among different orbitals with same spin. Due to the presence of the correlation effect, the quasi-particle band width (kinetic energy) is renormalized by factor Z_α^2 which is about 0.5 (0.7) for the a_{1g} (e'_g) state at $x=0.3$ (as shown in Fig.2). The same amplitude of renormalization is reported by ARPES [7].

Secondly, it has long been a controversial issue whether the e'_g states cross the Fermi level? To answer this question, the correlation renormalized level shift is crucial (as shown in Fig.2(c) the a_{1g} - e'_g level splitting Δ is much renormalized compared to LDA results). Unfortunately after including the correlation effect, two studies have been done, and conflicting results are drawn [10, 11] for $x=0.3$. It was recently pointed out by Marianetti *et al.* that the controversial is due to the different choice of crystal-field splitting in their tight-binding model [12]. To go further, in our studies, not only the crystal-field is treated parameter-free, but also the full charge self-consistency is achieved. To see the difference, we performed one-loop calculations (i.e. the charge-density is fixed to the LDA value and only Gutzwiller wave functions are optimized), then Marianetti's results are recovered, i.e. the e'_g pockets are not present for $x=0.3$. In addition, we also found that even for $x=0.2$ the e'_g pock-

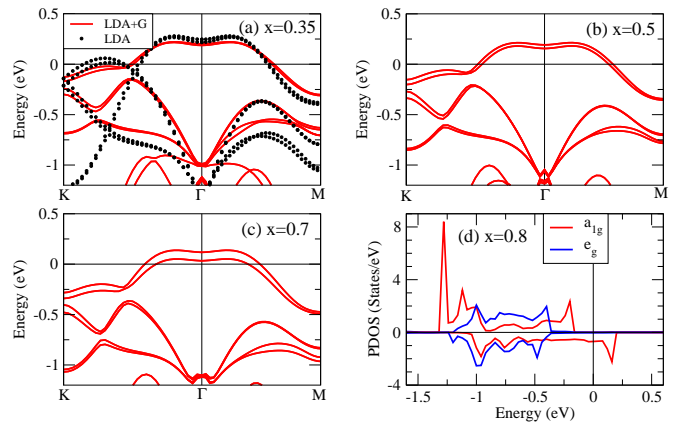


FIG. 3: The calculated band structure of Na_xCoO_2 for (a) $x=0.35$; (b) $x=0.5$; (c) $x=0.75$ in the NM state. (d) is the projected density of states (PDOS) for $x=0.8$ in the A-type AF state. $U=5.0\text{eV}$ and $J=1.0\text{eV}$ are used, and the spin-orbital coupling is included.

ets are not present in this one-loop calculation. However, after including the charge density self-consistency, the renormalization of level splitting are suppressed (see Fig.2(c)). As the results, we found that $x=0.3$ is the critical point, i.e. e'_g pockets are absent for $x > 0.3$ but present for $x < 0.3$. Our calculated quasi-particle bands (as shown in Fig.3 and discussed below) can be well compared with ARPES. Since with the interactions we used ($U=5.0\text{eV}$ and $J=1.0\text{eV}$) the static Hartree Fock shift is zero [11], the renormalized energy level shift here is fully contributed by the fluctuation effect. From Fig.2(c), we found that the Δ is peaked in the crossover region indicating that the inter-orbital fluctuation is the main reason for the renormalization effect on the energy levels.

Phase III: weakly correlated Stoner metal for $x > 0.6$. Clearly seen from the calculated density of states (Fig.3(d)), a sharp van-Hove singularity (VHS) is present near the a_{1g} band top-edge (due to the flat dispersion). For the Na rich side, the Fermi level is shifted close to the VHS, the Stoner instability make the system FM (in-plane). This conclusion is supported by the following facts for this region: (1) LDA works qualitatively well; (2) the magnetic solution only weakly depends on interaction strength U and J (see Fig.1); (3) calculated spin and charge fluctuation are all weak (Fig.2(b)). It is therefore suggested that strong correlation is not the driving force for the magnetic state, instead the VHS is responsible. Furthermore, we correctly predict that the A-type AF state is more stable than FM state (see the difference between solid and dashed lines in Fig.1). From Fig.3(d) for $x=0.8$, it is seen that spin moment mostly comes from the a_{1g} states, which aligns towards the z direction (inter-layer) of the crystal. According to the Goodenough-Kanamori rule, the exchange-coupling along z direction is dominated by AF super-exchange,

which stabilizes the A-type AF state. In fact, the estimated inter-layer exchange coupling (from the total energy difference between FM and A-AF solutions) is about $J_c=3.0$ meV, in good agreement with experimental results [3]. From itinerant FM theory, the size of spin moment may change with raising temperature, but in the presence of strong VHS near band edge, this possibility is prevented by the sharp density barrier. Indeed we found that the calculated moments of FM and A-type AF solutions are the same. Therefore, the a_{1g} moment will behave like localized spin as observed experimentally. In other words, the Curie-Weiss behavior in this region does not necessarily suggest the *enhanced correlation*.

Phase I: magnetic correlated metal: The main difference between phase I and II is that the e'_g band starts to go across the Fermi level and the e'_g hole pockets are present. Therefore phase I is effectively a multi-band system. In the meanwhile, the magnetic instability is recovered, and the system is stabilized in FM ground state. Several points should be addressed here to understand this phase: (1) in contrast to phase III, the FM state is slightly more stable than A-type AF state; (2) both e'_g and a_{1g} contribute to the spin moment, in other words, the stabilization of FM state is due to the enhancement of inter-orbit (rather than intra-orbit) spin fluctuation (Fig.2(b)), which is induced by the Hund's rule coupling; (3) strong correlation (rather than VHS) is responsible for the magnetic instability. It is interesting to note that the critical point $x \sim 0.3$ (boundary between phase I and II) is close to the doping level where superconductivity was observed. The experimental information for this region is quite limited and not conclusive due to the difficulty of sample preparation, our prediction should be evaluated by future experiments.

Finally, we show systematically in the Fig.3(a)-(c) the calculated quasi-particle band dispersion for $x=0.35, 0.5,$ and 0.7 after including the spin-orbital-coupling (SOC) effect. The overall picture can be nicely compared to ARPES data [7]. In particular, (1) the band width renormalization around factor of 2 is now obtained; (2) the e'_g Fermi surface pocket is absent; (3) the a_{1g} - e'_g anti-crossing along $\Gamma - K$ line is nothing but a effect of SOC, and the gap around 0.1 eV is comparable to experimental data [14].

In summary, using the recently developed LDA+Gutzwiller method, we are now able to calculate the ground state total energy of correlated

multi-orbital systems from *ab-initio* after taking into account the orbital fluctuation. The calculated phase diagram of Na_xCoO_2 establishes a general understanding for the physics behind. Most of the discrepancies between experiments and previous theories, such as the e'_g pocket, a_{1g} - e'_g anti-crossing, Curie-weiss behavior for $x > 0.5$, are self-consistently understood. Three distinct phase regions are identified, which is instructive to future experiments.

We acknowledge valuable discussions with H. Ding, and the supports from NSF of China (No.10334090, 10425418, 60576058), and that from the 973 program of China (No.2007CB925000).

-
- [1] M. L. Foo and, *et al.*, Phys. Rev. Lett **92**, 247001 (2004).
 - [2] Y. Wang, N. S. Rogado, R. J. Cava, N. P. Ong, Nature, **423**, 425 (2003).
 - [3] J. Sugiyama et al., Phys. Rev. B **67**, 214420 (2003); A.T. Boothroyd, et al., Phys. Rev. Lett. **92**, 197201 (2004); S. P. Bayrakci et al., Phys. Rev. Lett. **94**, 157205 (2005); L. M. Helme, Phys. Rev. Lett. **94**, 157206 (2005).
 - [4] K. Takada, H. Sakurai, E. T. Muromachi, F. Izumi, R. A. Dilanian, and T. Sasaki, Nature, **422**, 53 (2003).
 - [5] K.-W. Lee and W. E. Pickett, Phys. Rev. Lett. **96**, 096403 (2006); G. Gasparovic, and et.al, Phys. Rev. Lett. **96**, 046403 (2006).
 - [6] D. J. Singh, Phys. Rev. B **61**, 13397 (2000).
 - [7] H. B. Yang et al., Phys. Rev. Lett. **95**, 146401 (2005); D. Qian et al., Phys. Rev. Lett. **96**, 046407 (2006); D. Qian et al., Phys. Rev. Lett. **96**, 216405 (2006); D. Qian, L. Wray, D. Hsieh, L. Viciu, R. J. Cava, J. L. Luo, D. Wu, N. L. Wang, and M. Z. Hasan, Phys. Rev. Lett. **97**, 186405 (2006).
 - [8] P. Zhang and *et al.* Phys. Rev. Lett **93**,236402 (2004); P. Zhang and *et al.*, Phys. Rev. B **70**, 085108 (2004).
 - [9] M.Z. Hasan and *et al.* Phys. Rev. Lett **92**,246402 (2004); H.B.Yang and *et al.* Phys. Rev. Lett **92**,246403 (2004)
 - [10] S. Zhou and *et al.* Phys. Rev. Lett **94**,206401 (2005).
 - [11] H. Ishida, M. D. Johannes, and A. Liebsch, Phys. Rev. Lett.**94**, 196401 (2005).
 - [12] C. A. Marianetti, and *et al.*, Phys. Rev. Lett. **99**, 246404 (2007).
 - [13] X. Y. Deng, X. Dai, and Z. Fang, cond-mat/0707.4606.
 - [14] J. Geck, et. al. Phys. Rev. Lett. **99**, 046403 (2007).
 - [15] G. Kotliar, et al. Rev. Mod. Phys. **78**, 865 (2006).
 - [16] I. I. Mazin, and D. J. Singh, Phys. Rev. B **56**, 2556 (1997); Z. Fang, and Terakura, **64**, 020509 (2001).